Metastable-atom desorption and luminescence stimulated by low-energy electron impact on condensed Kr, Xe, and Xe/Kr films

A. Mann, G. Leclerc, and L. Sanche

Medical Research Council Group in the Radiation Sciences and Canadian Centre of Excellence in Molecular and Interfacial Dynamics, Faculté de Médecine, Université de Sherbrooke, Sherbrooke, Québec, Canada J1H 5N4
(Received 28 February 1992; revised manuscript received 22 June 1992)

Metastable-atom desorption and uv luminescence from thin films of Kr and Xe on Pt(111) stimulated by impact of monochromatic low-energy electrons ($E = 5-25$ eV, $\Delta E = 60$ meV) have been studied. For either pure rare-gas film, the excitation function of the total luminescence signal shows two broad peaks that are presumably related to the interplay between creation of excitons and free-electron–hole pairs. Metastable-particle desorption is very weak for pure Kr and not detectable for pure Xe over the entire range of electron energies. However, for 35-ML Kr films covered with 1-ML Xe (ML denotes monolayer), a considerable signal due to metastable-particle desorption is observed. The energy dependence of the signal in the 8–12.6-eV region leads to an interpretation of the desorption in the form of two different mechanisms with different thresholds. The first one is based on the creation of a Xe exciton in a Kr environment, while in the second scheme the excitation energy is transferred from a Kr bulk exciton to a Xe atom at the Kr-Xe interface. In both cases, repulsive Kr-Xe* interaction near the film surface is postulated to eject a metastable Xe* atom.

I. INTRODUCTION

Detailed information on the variety of relaxation processes that occur in condensed rare-gas films after electronic excitation has been obtained in recent years.[1–3] The energy of the stimulating ions, electrons, or photons is initially deposited in the film via creation of free excitons or free-electron–hole pairs. A number of pathways exists for the relaxation of these primary excitations as they diffuse through the crystal. Radiative decay of free excitons has been observed as a strong feature in high-quality Xe crystals.[4] Nonradiative quenching occurs at the metal–rare-gas interface, which is assumed to be a perfect sink for excitations.[5,6] However, excitons and holes can be trapped in a dimer configuration where the internuclear distance between two particular atoms is considerably reduced. Since the binding energies of R_2^* or R_2^+ (R denotes a rare-gas atom) and the lattice rearrangement around these centers are large, the so-called molecular self-trapped exciton (m-STE) state is localized.

A second trapping scenario features an excited atom in the center of a responding lattice (a-STE, or atomic STE). For Ne and Ar, the bulk electron affinity is negative (see V_0 in Table I) and the interaction of the outer electron with the electron cloud of the surrounding atoms is repulsive. A cavity is formed around the excited atom that is stable against both displacement and decay to the m-STE state. For Kr and Xe, having a positive bulk electron affinity, the nearest-neighbor distance contracts making the a-STE less stable against dimer formation.

Besides the spontaneous self-trapping of excitons even in a perfect lattice, trapping occurs at the site of crystal imperfections, impurities, and at the surface of the film. The different options for trapping type and site lead to a rich spectrum of vacuum-ultraviolet (vuv) luminescence, which has been described by several authors.[1–5,7–10] A compilation of the main luminescence features of Ar, Kr, and Xe films is given in Table II. In the case of Kr and Xe, the M band, corresponding to radiative decay of the vibrationally relaxed m-STE, dominates. The lighter rare

TABLE I. Energy values related to rare-gas films according to Schwentner *et al.* (Ref. 2). All values are in eV. E_{gap} is the band gap between the valence band and the conduction band. Only the lowest energies are given for the bulk (b) and the surface (s) excitons ($n = 1, j = \frac{3}{2}$). $\Delta E_{s.o.}$ is the spin-orbit splitting, V_0 the energy level of the bottom of the conduction band with respect to the vacuum level (negative value of the bulk electron affinity), and D_c the binding energy of an atom in the crystal. $E(^3P_2,\text{gas})$ gives the energy of the lowest metastable state of the free atom. The bottom line (Xe/Kr) refers to low-concentration Xe guest atoms in a Kr host matrix.

	E_{gap}	$E(1,\frac{3}{2},b)$	$E(1,\frac{3}{2},s)$	$\Delta E_{s.o.}$	V_0	D_c	$E(^3P_2,\text{gas})$
Ar	14.16	12.06	11.71	0.18	$+0.3$	0.080	11.55
Kr	11.61	10.17	9.95	0.69	-0.3	0.116	9.92
Xe	9.33	8.37	8.21	1.3	-0.4	0.170	8.31
Xe/Kr	10.1	9.01			-0.2		8.31

TABLE II. Prominent luminescence features of Ar, Kr, and Xe solids. In the description of the precursor, R refers to the respective rare-gas atom. Species labeled "gas phase" are ejected from the crystal prior to the decay. All transitions go to the respective ground state ($^1\Sigma_g^+$ or $^1S_0$). Concerning the bands, the given energy refers to the maximum of the feature and the width is the half-width at half maximum. The a and M bands may consist of several components with different crystal environments (trapping at defects, self-trapping in the perfect lattice). Less important features are omitted.

Luminescence feature	Precursor	Energy and width (eV)		
		Ar	Kr	Xe
M band	R_2^*, vibrationally relaxed, solid phase (m-STE)	9.72 ± 0.28^a	8.41 ± 0.21^a	7.14 ± 0.14^a
W band	R_2^*, vibrationally unrelaxed, probably gas phase	$11.38\pm0.14^{b,c}$		
a band	R^*, solid phase (a-STE)	11.55 ± 0.02^b		
$^{3,1}P_1$ lines	R^*, gas phase, optically allowed transition	$11.62;11.82^d$		
Free-exciton line	free excitons ($n=1$, $j=\frac{3}{2}$, bulk)		10.14^d	8.35^d

[a]From Ref. 3.
[b]From Fig. 2 of Ref. 9.
[c]Unsymmetrical peak.
[d]From Ref. 8.

gases Ne and Ar show additional features, such as the a band(s) after trapping in a-STE states; the W band, which reflects the decay of vibrationally unrelaxed dimers ejected into vacuum;[10] and sharp lines attributed to emission from desorbed excited atoms. Two mechanisms for the desorption of particles have been identified: (i) the decay of an m-STE state at or close to the surface to a repulsive state (e.g., ground state), and (ii) the ejection of an atomic or molecular STE localized at the surface due to the repulsive interaction with the neighbors ("cavity expulsion," in Ne and Ar).

Recently, very detailed studies have been performed with Ar films concerning the desorption of Ar,[11] Ar*,[12,13] and Ar$_2^*$.[10] In the present paper, we report on luminescence induced by the impact of monochromatic low-energy (5–25 eV) electrons on multilayer films of Kr and Xe and on the desorption of metastable atoms from Xe-covered multilayer Kr films under similar conditions. We focus on the heavier rare gases Kr and Xe, where some basic differences in the desorption behavior can be expected compared to Ar. Not only does the positive electron affinity inhibit the cavity-expulsion mechanism, but the energy of the $n=1$ surface exciton $E(1,\frac{3}{2},s)$, which is a probable precursor to the desorption, is simply too low to allow the desorption of a metastable atom. The desorption requires a minimum energy equal to the sum of the energy of the lowest metastable state in the gas phase [$E(^3P_2$, gas)] and the binding energy of the atom to the crystal (D_c). Thus,

$$\Delta E = E(1,\tfrac{3}{2},s) - E(^3P_2,\text{gas}) - D_c < 0$$

for Kr and Xe (see Table I). In this context, the study of Kr films with a Xe top layer appears interesting, since an estimate with the values of Table I gives $\Delta E > 0$. Moreover, the energy deposition in the films by means of a variable-energy monochromatic electron beam allows a close look at particular features of the energy dependence of the excitation eventually leading to luminescence and metastable-particle desorption.

II. APPARATUS

The electron-energy dependence of the luminescence and the metastable-particle yield was recorded with an apparatus described previously.[13–15] It consists essentially of an electron monochromator, a cryogenically cooled Pt(111) target, and a system capable of detecting metastable particles and photons. The electron monochromator provides a collimated beam with an intensity of 1 nA having an energy resolution of 60 meV. The electron energy ranges from 1 to 100 eV with an estimated uncertainty of less than 0.1 eV. Owing to the use of double-zoom focusing optics at the exit of the monochromator, the electron current is constant within 30% over the entire energy range as deduced from the transmission to the pure crystal. Target films are condensed onto the Pt(111) crystal held at a temperature of 20 K. The thickness of a film is estimated by the amount of gas introduced. It is calibrated with respect to the quantity of gas required to build the first layer as inferred from temperature-programmed desorption.

The detection system is a low-energy-electron-diffraction–type configuration with four spherical grids, a block of three microchannel plates (MCP's), and a position-sensitive anode. In the present context, the grids are biased to reject charged particles, and only photons or metastable particles with an energy above about 7–8 eV are counted. This threshold value is estimated from the lowest electron energy producing a signal for various target species. A distinction between photons and metastable particles is possible in the pulsed electron-beam mode by measuring the time delay between the electron pulse and the detection event. For the present experiments, the pulse width is generally set to 25 μs in order to have a high signal intensity. The signal during the first 30 μs (including 5 μs for delayed processes) is due to photons, while any signal thereafter originates from the detection of metastable atoms. The usual length of the pulse-and-detection period is 600 μs. In various tests it has been checked that no metastable particles interfere with the photon signal, i.e., that the photon emission is not delayed by more than 5 μs and that the flight time of

the metastable particles generally lies between 30 and 600 μs (5 meV $< E <$ 2 eV for Xe*). Due to the low counting rate for Kr and Xe films, the signal is integrated over the whole anode area, and no information on the angular distribution of the signal is obtained. The detector covers an angular range of $\pm 35°$ with the normal of the target surface being tilted by $18°$ with respect to the electron-beam axis and the normal of the detection plane. The data-collection time with a given film is limited due to charging of the film and condensation of particles from the background ($p_0 = 2 \times 10^{-8}$ Pa). Normal collection cycles last for 30–60 min.

III. RESULTS AND DISCUSSION

A. Pure films

1. Luminescence

Condensed films of either pure Kr or pure Xe with a thickness of about 25 ML (monolayers) have been studied in the first phase of the present experiments. The uv-photon signal as function of the incident-electron energy is depicted in Fig. 1. The given count rate refers to non-pulsed electron impact and is considerably higher for Kr than for Xe, but no correction for the relative sensitivity of the detection system has been made. Referring to the work compiled in Table II, the photon signal is interpreted to be emission from free-exciton states and relaxed m-STE states (M band). The W band, the a band, and the free-atom emission lines are very weak or absent in Kr and Xe. In a simple picture, this behavior can be attributed to the negative value of V_0 meaning no cavities and no cavity expulsion of excited atoms or dimers.

For both rare-gas films, the photon signal shows a strong dependence on the electron energy with two regions of pronounced photon yield being discernible. Referring to the vacuum level, thresholds are expected at electron energies E_e of

$$E_e = mE_{\text{exc}} + V_0, \quad m = 1, 2, \ldots .$$

These values assume the (multiple) excitation of the lowest exciton state of energy E_{exc}, and the scattering of the incident electron to the bottom of the conduction band, giving a total available energy of $E_e - V_0$. The lines in Fig. 1 indicate the threshold electron energies for the mentioned processes as deduced from the values given in Table I. The first peak has its onset near the energy for exciting the first exciton and its width (full width at half maximum) is about 4.5 eV for Kr and 3.0 eV for Xe. The second feature appears broader and with less maximum intensity; it is attributed to the excitation of two excitons.

The exact analysis of the energy dependence of the luminescence signal in Fig. 1 seems to be beyond present-day possibilities. The matrix elements for exciton creation by electron impact and the band structures of initial and final states are crucial in determining the signal intensity. An exact calculation has to respect energy and momentum conservation and take into account multiple electron scattering as well as exciton diffusion and in-

teraction with phonon modes. We will therefore proceed with this discussion on a qualitative basis.

The density of states for the extra electron in Kr and Xe is considerably structured,[16] but no similar structure is resolved in Fig. 1, although the energy resolution of the electron beam would be sufficient. Due to the width of the valence band (2.3 eV for Kr, 3.0 eV for Xe; Ref. 2), the energy loss of the scattering electron is not precisely defined, and we expect that a smooth function describes the effect of the electronic band structures of the crystal. Another factor controlling the transition probability is given by the matrix elements for exciton creation by electron impact. They are reflected in the electronic excitation functions of gas-phase Kr and Xe, which exhibit a monotonically increasing function of energy[17] except for narrow peaks related to anion states.[18]

After these remarks, the decrease of the luminescence yield starting a few eV above threshold is perhaps surprising. A probable explanation is obtained by considering the influence of a concurrent process: the excitation of free-electron–hole pairs that do not recombine significantly and thus do not enter into the exciton-decay
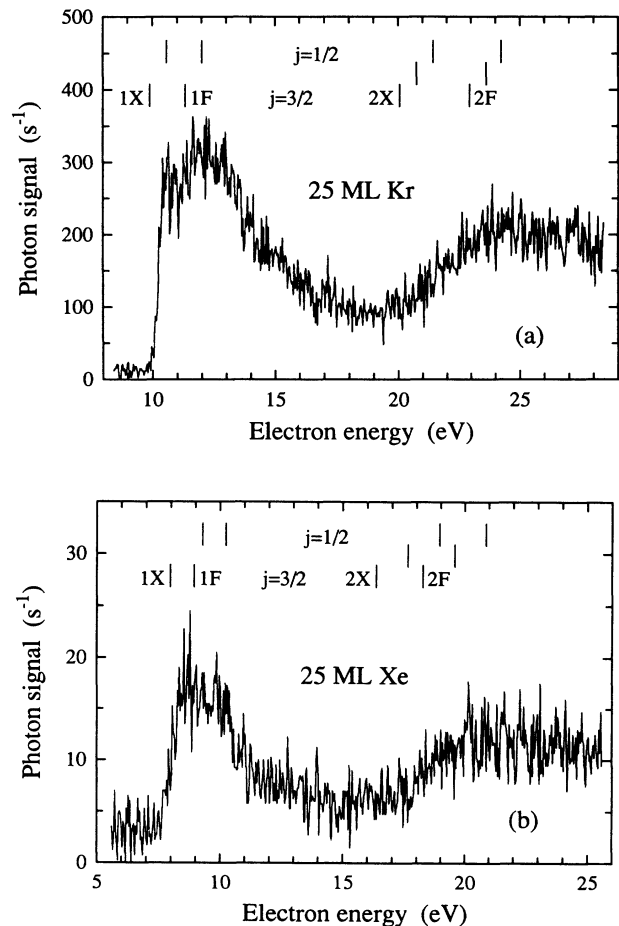

FIG. 1. uv-photon signal from (a) a 25-ML Kr film and (b) a 25-ML Xe film on Pt(111) as function of incident-electron energy. The lines indicate the values of $mE(n = 1, b) + V_0$ and $mE_{\text{Gap}} + V_0$, $m = 1,2$, for the $j = \frac{3}{2}$ and $\frac{1}{2}$ systems (X denotes the $n = 1$ bulk exciton and F the free-electron–hole pair).

scheme. The energetic threshold of this process is given by $E_{gap} + V_0$ corresponding to one hole at the top of the valence band and two electrons at the bottom of the conduction band. The electron and the hole move freely in the crystal and have various relaxation channels besides the radiative recombination, especially quenching at the film-metal interface. If the density of electrons and holes is high, the recombination may be seen as the precursor of essentially all sputtering and luminescence events (Ref. 6 for Ar), but in the low-density limit the quenching dominates. Due to the density of final states, the probability for the creation of a free-electron–hole pair grows faster with energy than the probability for the creation of an exciton. Consequently, at some point above $E_{gap} + V_0$ the former process starts to dominate. In the crystal, the competition is enhanced due to multiple scattering, and the luminescence drops off. The evident difference in the peak width between Kr and Xe is correlated with the different exciton binding energy, which connects the thresholds for the two mentioned processes. Following this argument, the second feature in each of the luminescence spectra in Fig. 1 should have about twice the width of the first peak, in rough agreement with the experimental result.

The above discussion applies to both the $j = \frac{3}{2}$ and the $\frac{1}{2}$ systems. Between the two systems, the energy values for excitons and band gap differ by the value of the spin-orbit splitting given in Table I. Both contributions should be similar and the spin-orbit splitting is contained in the width of the peaks.

Comparable results on low-energy electron stimulation of uv luminescence exist only for Ar films. Möller et al.[19] have been monitoring the luminescence yield of an Ar film irradiated by synchrotron radiation. In their experiment, a photoelectron is created in the first step, which subsequently loses energy in electron-electron scattering processes. Steps in the luminescence yield are found at excitation energies

$$E_{photon} = E_{gap} + mE_{exc}, \quad m = 1, 2, 3$$

corresponding to the thresholds for creating m excitons and one free-electron–hole pair. These values resemble the threshold electron energies with respect to the vacuum level found in this work. It appears that the photoelectron is not scattered back to a bound-exciton state, but remains free after losing energy in the scattering process. Exciton creation with recombination would show steps in the luminescence signal at $(m + 1)E_{exc}$. Therefore, in both experiments the threshold is defined by the process leaving the electron at the bottom of the conduction band.

Coletti et al.[8] directly measured the luminescence yield from Ar films for incident electrons in the energy range 0–80 eV. Moreover, they presented excitation functions for the main luminescence signals (M band, a and, $^3P_1$ line, and W band; see Table II). The general feature of all these spectra is the onset at about the energy value for the creation of an exciton, while a structure (dip) at the energy value corresponding to the creation of two excitons is observed only for signals related to processes at the surface ($^3P_1$ line and W band). The excitation functions for the M band and the a band monotonically increase over the whole energy range. Coletti et al. do not provide an interpretation of this behavior, but in light of the discussion given above and assuming a significant electron-hole recombination in the experiment of Coletti et al. ($j < 1 \ \mu A/mm^2$), the difference in the excitation functions for bulk- and surface-related processes can be rationalized by assuming that excitons are more readily trapped at the surface than holes. Thus, depending on the excitation energy, the relative number of excitons and holes changes and, with it, the relative intensity of bulk- and surface-related emission. The difference between the M-band signal of Coletti et al. and our luminescence signal, which is assumed to be mostly due to M-band emission, is therefore related to the different density of free electrons and holes in the film. Without recombination, as in the present experiment and a previous one[14] on Ar* desorption, all signals (bulk or surface related) exhibit the dip in the excitation function.

2. Metastable-particle desorption

Over the range of incident-electron energy, 5–25 eV, no metastable-particle desorption is observable for Xe. From the Kr films, the desorption signal is very low, with a plateau in the 11–12-eV region. With the same experimental setup, the metastable-particle signal from Ar films was strong enough to allow the determination of five desorption components.[13] Evidence for different desorption behaviors of the lighter and heavier rare-gas solids can be deduced from the luminescence features after low-energy electron impact.[8] In contrast to the case of Ne and Ar films, the absence of surface-related emission from Kr and Xe films rules out the ejection of any excited atoms or dimers. These considerations are corroborated by photon-stimulated-desorption (PSD) experiments[9] with synchrotron radiation in the 8–30-eV range. Metastable particles have been detected for Ne and Ar films, but not for Kr and Xe.

A somewhat controversial result has been reported by Arakawa et al.[20] using an electron beam of $E = 200$ eV for the excitation of rather thick films (1000 ML). These authors give time-of-flight (TOF) spectra for metastable particles from Ar, Kr, and Xe films. Whereas the TOF spectrum for Ar shows two peaks corresponding to Ar* particles with a kinetic energy of 0.04 and 0.4 eV in accordance with other work (e.g., Ref. 13), the spectra for Kr and Xe exhibit only one peak each at relatively short flight times. Its interpretation as a Kr* or Xe* signal gives kinetic-energy (KE) values of 0.7 and 1.5–2.0 eV, respectively. In the case of Xe, Arakawa et al. mention that the signal intensity is rather low and strongly depends on conditions favorable for H_2 adsorption, so that contamination could have been detected or involved in producing the Xe* signal. In the case of Kr, however, there are no such restrictions and Arakawa et al. additionally present the signal intensities for various values of the film thickness. It appears that the signal is small at 30 ML and saturates only for values above about 100 ML. Since the Kr*-signal intensity amounts to only 1%

of the value for the fast Ar* component,[20] it seems possible that the conditions in the experiment of Arakawa et al. (high electron current of 0.5–10 μA, thick films) have been favorable enough in comparison with the other mentioned experiments to observe the Kr* desorption. In the present experiment, high sensitivity is obtained by means of the large detection area. Our observation of a weak Kr* signal supports the results of Arakawa et al. and establishes that the Kr* signal is present at low impact energies. It arises form some dissociative electronically excited states in the solid (probably some higher excited Kr_2^{**}) which provide sufficient KE to Kr* atoms to allow their ejection into vacuum. Such dissociative states are created by electrons with a KE of about 11 eV or more. On the other hand, the absence of the slow-Kr* signal in the TOF spectrum of Arakawa et al. agrees with the missing a-STE states in Kr solids due to the negative value of V_0.[7] This simple picture based on electron affinity has been corroborated in recent molecular-dynamics simulations for Kr.[21] Similar calculations already predicted[22] the three observed[13] slow-Ar* desorption components from Ar films.

B. Monolayer-multilayer Xe/Kr films

Since the pure Kr and Xe films show little or no metastable-particle signal, an experiment with a 35-ML Kr film covered by 1 ML Xe appeared to be useful for a further understanding of the ejection mechanisms. Taking the energy value of the lowest Xe exciton in a Kr matrix (9.01 eV; see Table I for all energy values mentioned below) and an estimated binding energy of 0.14 eV (average between the Kr and the Xe value), the energy balance for desorption of Xe* in the lowest metastable state gives a positive value of about 0.56 eV to be shared between the desorbed particle and the lattice. Starting with the Kr bulk exciton, even more surplus energy is available (1.7 eV), but desorption of Xe* depends on the existence of an effective mechanism for transferring the electronic energy to kinetic energy of the Xe* atom. The cavity expulsion, which is expected to work for Xe in Ar and Kr in Ar ($V_0=0.3$ eV for both cases; see Ref. 2), can be ruled out in the case of Xe in Kr due to the positive electron affinity ($V_0=-0.2$ eV).

1. Electron-energy spectra

Figure 2 shows the luminescence signal and the metastable-particle signal from a (1 ML Xe)/(35 ML Kr) film for electron energies between 6.6 and 12.6 eV. Both signals have about equal intensity, which is much less than the luminescence from the pure Kr film, but comparable to that from the pure Xe film. A plateau is reached in both curves at 10.2 eV, similar to Fig. 1(a), and probably related to the excitation of bulk excitons in Kr.

The three vertical lines in Fig. 2 indicate three electron-energy values that seem meaningful in the present context. The first line is at the threshold for creating a (bulk) exciton in a Xe film $[E(1,\frac{3}{2},b)+V_0=7.97$ eV; for the sake of simplicity, only the values for bulk excitons are considered]. From Fig.
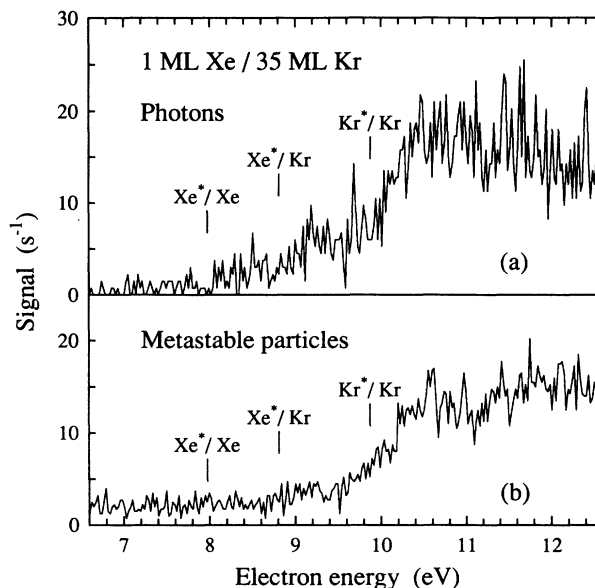

FIG. 2. Incident-electron energy dependence of (a) the uv-photon signal and (b) the metastable-particle signal from a 35-ML Kr film on Pt(111) covered by 1 ML Xe. The lines indicate the values of $E(n=1, j=\frac{3}{2}, b)+V_0$ for pure Xe, Xe in Kr, and pure Kr.

2(a), this value appears to be also the threshold for the photon signal from the two-layer film. This relation is similar to the case of a pure Xe film as depicted in Fig. 1(b). Since only abut 1 ML of Xe is deposited, the signal intensity in the threshold region is now much lower than with the pure film. The threshold for the metastable-particle signal is found at considerably higher energy in the vicinity of the threshold for Xe*/Kr creation (8.81 eV). The latter value probably depends on the specific concentration and location of Xe and Kr atoms around the excited atom and is regarded only as a rough estimate for describing the observed onset. A different interpretation could be based on the creation of a free-electron–hole pair in Xe (threshold at 8.9 eV), but from the results on pure films it has been concluded that electron-hole recombination does not significantly contribute to the metastable-atom signal in the present experiment. The third energy value (9.87 eV) in Fig. 2 corresponds to the excitation of a Kr bulk exciton and is correlated with the onset of the region of maximum signal intensity for both the photon and the metastable-particle signal.

The effect of the thickness of the Kr film is evident form the two spectra in Fig. 3, where the total signal from Xe-covered films with either 35- or 4-ML of Kr is depicted. Due to the unpulsed electron beam, the signal-to-noise ratio is much better than in Fig. 2. Below 8.9 eV, the two signals are essentially identical. Both curves have a threshold at about 8.0 eV and rise linearly up to 8.9 eV. While curve b continues to rise with constant slope up to 10.6 eV, the slope of curve a increases slightly at 8.9 eV and again, more strongly, between 9.7 and 10.0 eV. At the upper limit of this spectrum, a region of constant signal is indicated, with the 35-ML signal having 5 times the intensity of the 4-ML signal. Interestingly
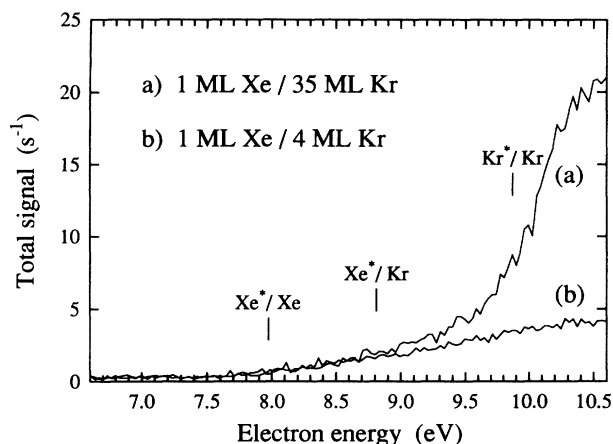
A. MANN, G. LECLERC, AND L. SANCHE

FIG. 3. Total signal (uv photons and metastable particles) from (a) a (1 ML Xe)/(35 ML Kr) film and (b) a (1 ML Xe)/(4 ML Kr) film, both on Pt(111), as a function of the energy of the incident electron. The lines indicate the values of $E(n = 1, j = \frac{3}{2}, b) + V_0$ for pure Xe, Xe in Kr, and pure Kr.

enough, the same two energy values observed as thresholds in the photon signal and in the metastable-particle signal (Fig. 2) appear again as the general onset and as the onset of the difference of the two curves in Fig. 3. Time-resolved spectra have been taken to identify the signal from the (1 ML Xe)/(4 ML Kr) film, and while a weak photon signal is detectable, any metastable-particle desorption is buried in the noise. The ratio of photon to metastable-particle signal is estimated to be at least 5 over the energy range of Fig. 2. Thus it appears from Figs. 2 and 3 that metastable particles are desorbed only for electron energies above about 8.8 eV and only from films with a "thick" Kr layer.

2. Discussion

The interpretation of the signal is arranged according to the three energy regions described before. In the first region, the same mechanism leads to luminescence as in the pure Xe film. One may ask about the nature of pure Xe-type excitons in a film containing only a single monolayer of Xe. However, the microscopic structure of the two-layer film is uncertain. We do not expect a perfect monolayer coverage of a perfect Kr crystal, but rather a Kr surface with vacancies, dislocations, and steps, covered by a locally varying number of Xe atoms. So, Xe-on-Xe surface-type excitons may be created by the electrons, thus accounting for the threshold of the photon signal around 8.0 eV.

In the second energy region of Fig. 2, metastable-particle desorption is observed. From the available energy it is obvious that the detected particles are Xe* atoms. The most convincing scenario starts with the excitation of a Xe atom in the neighborhood of a Kr atom in the form of an excitation center Kr-Xe*. This initial state has an estimated energy of 9.0 eV which is higher than both the energy of the crystal with a relaxed Kr-Xe* m-STE center (≈ 7.8 eV, Ref. 1) and the energy of a desorbed Xe* atom $[E(^3P_2, \text{gas}) + D_c = 8.45$ eV]. From a simple potential-energy picture (Fig. 4), motion in both
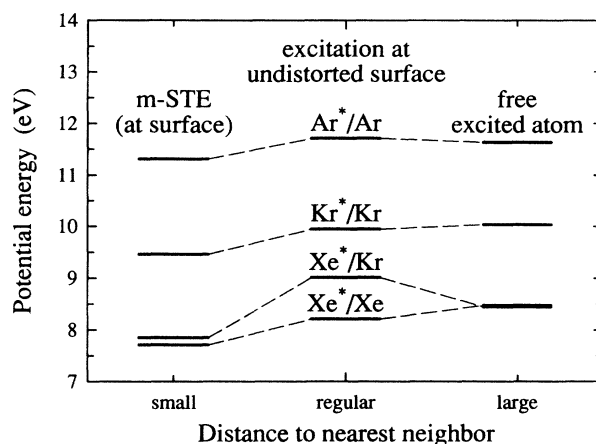
FIG. 4. Potential-energy values for excitations at the surface of rare-gas crystals. Three locations of the excited atoms are indicated schematically. Initially, an atom in an undistorted surface is presumably excited to the lowest surface-exciton state (Table I; bulk value for Xe*/Kr). The free-atom values ($^3P_2$ excitation energy plus binding energy) are also given in Table I. The potential-energy values for the relaxed m-STE are obtained from Ref. 1 as the sum of the M-band energy, the dissociation energy of the ground-state dimer, and the binding energy. Although the Xe*/Kr potential for the undistorted lattice is only approximate, a different desorption behavior for Ar*/Ar and Xe*/Kr compared to Kr*/Kr and Xe*/Xe can be rationalized.

"directions" is possible. Inward motion results in a vibrationally relaxed heteronuclear m-STE that eventually decays to the repulsive ground-state by emitting a photon of about 7.4 eV (Ref. 1). Outward motion along a repulsive potential-energy curve leads to acceleration of both the Kr and the Xe*. According to the mass ratio and neglecting interaction with the lattice, an estimate of 220 meV for the kinetic energy of the desorbing Xe* atom is obtained. This scenario defines the threshold for the desorption of an excited Xe atom from the Xe/Kr film. However, the intensity is much less than in the third region, and even further reduced in the vicinity of the metal, as seen in Fig. 3 from the difference between the films containing 35- and 4-ML Kr layers.

It appears from Fig. 4 that a similar process is possible for pure Ar films, but not for pure Kr and Xe films. We expect a previously[13] observed Ar* desorption component with a mean kinetic energy of 85 meV to be related to this mechanism. While the cavity expulsion assumes an average interaction potential with all neighbors,[7,22] the presently proposed mechanism relies on the preservation of a repulsive dimer interaction with a certain neighbor similar to the attractive interaction leading to m-STE states. Consequently, the kinetic energy of the desorbed particle should be higher, but for Ar films, where both processes are possible, the intensity is lower for the dimer repulsion than for the cavity expulsion.[13]

In the third energy region, obviously Kr bulk excitons are created by electron impact, and again luminescence and metastable-particle desorption are observed. As for the pure Kr film, free-exciton and m-STE decay are expected to contribute to the luminescence signal. Addi-

tionally, since the Kr M band (8.4 eV) overlaps with the Xe exciton energies, excitation transfer from Kr to Xe is possible via dipole-dipole interaction (Förster-Dexter mechanism; see Ref. 2 and references therein). As mentioned before, the energy of a Xe exciton is too low for desorption of Xe* atoms and finally a photon, most probably from the Xe M band (7.1 eV) or the Xe-Kr M band (7.4 eV), will be emitted. Thus, the excitation transfer from Kr to Xe shifts the photon energy downward, and the signal will decrease severely owing to the energy-dependent detection efficiency of the MCP. Comparing the photon signal from the pure Kr film [Fig. 1(a)] and the Xe-covered Kr film [Fig. 2(a)], the Förster-Dexter mechanism appears to be very efficient for Xe/Kr two-layer films.

The detected metastable particles in the third energy region are most probably Xe* atoms, since the Kr* desorption signal from the pure Kr film is much smaller and should be further reduced by the Xe cover layer. A possible desorption mechanism features the formation of a Kr*-Xe m-STE, but since the excitation is initially with the Kr atom, the potential is different from the previously mentioned Kr-Xe* potential. During the relaxation of the Kr*-Xe m-STE, multiple curve crossings with repulsive Kr-Xe* potential-energy curves occur, and the transition can easily lead to desorption of Xe*. Since the dissociation energy depends on the amount of energy released into lattice relaxation by the time of the transition, we expect a broad kinetic-energy distribution around 0.4 eV.

Some experimental results on desorption and luminescence from covered rare-gas films have been reported previously in the literature. An enhanced excitation trapping probability at the surface was found by Reimann et al.[6] for monolayer coverages of O_2 on Ar films. Radiative and nonradiative decay from transient molecular excited states like Ar-O (and Ar-N from N_2-covered Ar films) were discussed, but a detailed microscopic description could not be obtained. Similar experiments by Hudel et al.[11] stressed the role of excited compounds of Ar and some of the intentionally added surface impurity molecules (N_2,NO,O_2), indicating direct particle ejection after the decay of Ar-NO and Ar-O_2. Only a qualitative picture of the desorption at impurity sites exists at present, but we hope that further experimental and theoretical work, perhaps on the relatively simple Xe/Kr system, will contribute to a better understanding.

IV. SUMMARY

With a monochromatic beam of low-energy electrons, excitation functions have been recorded for the electron-

stimulated luminescence and metastable-particle desorption from rare-gas (Kr,Xe) condensed films. Broad structures a few electron volts wide appear in the luminescence signal. Their onsets are associated with the creation of one and two excitons. A process that competes with luminescence after exciton formation is the creation of free-electron–hole pairs, since with the low-intensity irradiation of the present experiment the recombination rate of electrons and holes is small. The difference between the threshold values of the two types of excitation, i.e., the exciton binding energy, is correlated with the width of the observed structures (see Fig. 1).

Metastable-particle desorption with an intensity similar to the luminescence signal is detected only for Xe-covered multilayer Kr films (1 ML Xe, 35 ML Kr). The control of the electron energy allows us to determine thresholds and structures in the 8–12-eV region. In addition to the threshold values known for exciton creation in the pure films, a new threshold related to metastable-particle desorption appears around 8.8 eV. In simple, two-particle potential-energy curves, two mechanisms can be described leading to the desorption of Xe* atoms from Xe-covered multilayer Kr films. The threshold process is proposed to be the creation of a Xe exciton at the Xe-Kr interface followed by repulsive interaction of a Kr-Xe* complex; the energy balance allows for desorption of the Xe* atom. The same picture is applicable to pure rare-gas crystals, but while for Ar a corresponding desorption component is expected, the energy balance prohibits metastable-atom desorption from Kr and Xe crystals. Confirming experimental results have been obtained previously[13,20] and in the present work.

A much higher desorption intensity is observed in the monolayer Xe–multilayer Kr experiment if the excitation energy is high enough to create Kr bulk excitons. The efficiency depends on the thickness of the Kr film. The scenario leading to Xe* atom desorption features the Kr bulk exciton diffusing to the surface and transferring excitation energy to a Xe atom via the sequence Kr*-Xe→Kr-Xe*. Multiple curve crossings between attractive Kr*-Xe and repulsive Kr-Xe* potential-energy curves are expected. This mechanism gives rise to the desorption of fast excited particles. It is similar to the one proposed for the fast Ar* from Ar (Refs. 12, 13, and 20) and the Kr* from Kr (Ref. 20) signals.

[1] I. Ya. Fugol', Adv. Phys. 27, 1 (1978).

[2] N. Schwentner, E.-E. Koch, and J. Jortner, Electronic Excitations in Condensed Rare Gases (Springer-Verlag, Berlin, 1985).

[3] G. Zimmerer, in Excited-State Spectroscopy in Solids, edited by U. M. Grassano and N. Terzi (North-Holland, Amsterdam, 1987).

[4] T. Kloiber, H.-J. Kmiecik, M. Kruse, M. Schreiber, and G. Zimmerer, J. Lumin. 40&41, 593 (1988).

[5] A. Hourmatallah, F. Colletti, and J. M. Debever, J. Phys. C 21, 1307 (1988).

[6] C. T. Reimann, W. L. Brown, and R. E. Johnson, Phys. Rev. B 37, 1455 (1988).

[7]F. Colletti, J. M. Debever, and G. Zimmerer, J. Phys. (Paris) Lett. **45**, 467 (1984).

[8]F. Colletti, J. M. Debever, and A. Hourmatallah, Phys. Scr. **35**, 168 (1987).

[9]T. Kloiber and G. Zimmerer, Radiat. Effects Defects Solids **109**, 219 (1989).

[10]C. T. Reimann, W. L. Brown, D. E. Grosjean, and M. J. Nowakowski, Phys. Rev. B **45**, 43 (1992).

[11]E. Hudel, E. Steinacker, and P. Feulner, Phys. Rev. B **44**, 8972 (1991).

[12]I. Arakawa and M. Sakurai, in *Desorption Induced by Electronic Transitions, DIET IV*, edited by G. Betz and P. Varga (Springer-Verlag, Berlin, 1990).

[13]G. Leclerc, A. D. Bass, A. Mann, and L. Sanche, Phys. Rev. B **46**, 4865 (1992).

[14]G. Leclerc, A. D. Bass, M. Michaud, and L. Sanche, J. Electron Spectrosc. Relat. Phenom. **52**, 725 (1990).

[15]G. Leclerc, Ph.D. thesis, Université de Sherbrooke, 1991.

[16]M. Michaud, P. Cloutier, and L. Sanche, Phys. Rev. B **44**, 10485 (1991).

[17]N. J. Mason and W. R. Newell, J. Phys. B. **20**, 1357 (1987).

[18]S. J. Buckman, P. Hammond, G. C. King, and F. H. Read, J. Phys. B **16**, 4219 (1983).

[19]H. Möller, R. Brodmann, G. Zimmerer, and U. Hahn, Solid State Commun. **20**, 401 (1976).

[20]I. Arakawa, M. Takahashi, and K. Takeuchi, J. Vac. Sci. Technol. A **7**, 2090 (1989).

[21]W. T. Buller and R. E. Johnson, Phys. Rev. B **43**, 6118 (1991).

[22]S. Cui, R. E. Johnson, and P. T. Cummings, Phys. Rev. B **39**, 9580 (1989).